BBA - Biomembranes 1861 (2019) 1037–1048

Contents lists available at ScienceDirect

BBA - Biomembranes

journal homepage: www.elsevier.com/locate/bbamem

Regulation of intracellular pH by electrogenic Na+/HCO3– co-transporters in embryonic neural stem cell-derived radial glia-like cells

Tommy Nordström[a,*], Leif C. Andersson[b], Karl E.O. Åkerman[a]

[a] Faculty of Medicine, Medicum, Division of Physiology, PO Box 63, University of Helsinki, FIN-00014 Helsinki, Finland
[b] Department of Pathology, Haartmaninkatu 3 (PB 21), University of Helsinki, 00014 Helsinki, Finland

ARTICLE INFO

Keywords:
Neurosphere
Stem cell
Na+/HCO3– co-transporter
pH
Hyperpolarization
Calcium

ABSTRACT

A stroke causes a hypoxic brain microenvironment that alters neural cell metabolism resulting in cell membrane hyperpolarization and intracellular acidosis. We studied how intracellular pH (pH_i) is regulated in differentiated mouse neural progenitor cells during hyperpolarizing conditions, induced by prompt reduction of the extracellular K^+ concentration. We found that the radial glia-like population in differentiating embryonic neural progenitor cells, but not neuronal cells, was rapidly acidified under these conditions. However, when extracellular calcium was removed, an instant depolarization and recovery of the pH_i, back to normal levels, took place. The rapid recovery phase seen in the absence of calcium, was dependent on extracellular bicarbonate and could be inhibited by S0859, a potent Na/HCO3 cotransporter inhibitor. Immunostaining and PCR data, showed that NBCe1 (SLC4A4) and NBCn1 (SLC4A7) were expressed in the cell population and that the pH_i recovery in the radial glial-like cells after calcium removal was mediated mainly by the electrogenic sodium bicarbonate transporter NBCe1 (SLC4A4). Our results indicate that extracellular calcium might hamper pH_i regulation and Na/HCO3 cotransporter activity in a brain injury microenvironment. Our findings show that the NBC-type transporters are the main pH_i regulating systems prevailing in glia-like progenitor cells and that these calcium sensitive transporters are important for neuronal progenitor cell proliferation, survival and neural stem cell differentiation.

1. Introduction

Severe local ischemia after a stroke or brain trauma is caused by impaired blood flow to a specific brain area. During ischemia, significantly increased neurogenesis in the subventricular zone is initiated suggesting the presence of an inherent mechanism for repair [1,2]. Short, intermittent hypoxia also enhances neurogenesis and improves cognitive functions [3]. Moreover, it has been shown that neural progenitor cells (NPC) migrate to the injured area in ischemia [4–6], suggesting that specific and powerful chemo-attractant signals are provided by the injured tissue. The differentiation, viability and proliferation of NPCs are considerably enhanced under hypoxic conditions [7–9].

Stem cell-derived radial glial cells play an important role after a brain injury by mediating neuronal guidance during the recovery process. In a previous study, we used mouse neurosphere cultures as a model system, and observed that hypoxia (experimental ischemia) induced a prompt hyperpolarization in the differentiated neuronal cell population. Additionally, we found that the cells in the vicinity of the neurosphere body, consisting mainly of glia-like progenitor cells and radial glial cells, responded to experimental ischemia by intracellular acidification [10].

Hypoxia-induced intracellular acidification has been shown to be protective in several cell systems. In cardiomyocytes, prolongation of post-ischemic intracellular acidosis (delay in the recovery of intracellular pH during initial reperfusion) can limit infarct damage by inhibiting mitochondrial permeability transition and proteolysis and spread of injury during the first minutes of reflow [11]. Mild extracellular acidosis has been shown to induce intracellular acidification in neurons and to protect against ischemic injury and *N*-methyl-D-aspartate (NMDA) type glutamate receptor-induced cytotoxicity in neurons [12–14]. A variety of ion channels, responsible for neuronal signaling and glial-neuron cell communication, have previously been shown to be affected by changes in both intracellular and extracellular pH [15,16]. On the contrary, glial acidosis has been shown to trigger glial glutamate release and neuronal cell death [17].

In this paper, we used BCECF (2′,7′-Bis-(2-Carboxyethyl)-5-(and-6)-Carboxy-fluorescein) to monitor pH_i, and studied how glia-like

* Corresponding author.
E-mail address: tommy.nordstrom@helsinki.fi (T. Nordström).

https://doi.org/10.1016/j.bbamem.2019.03.007
Received 1 November 2018; Received in revised form 11 March 2019; Accepted 14 March 2019
Available online 16 March 2019

progenitor cells respond to hyperpolarizing conditions induced by reduced extracellular K^+ concentration. Our results show that glia-like cells derived from neural stem cells are rapidly acidified under hyperpolarizing conditions. The role of Na + /HCO3– co-transporters and extracellular calcium for the hyperpolarization induced acidification and recovery from acidosis in radial glia-like cells is discussed.

2. Methods

2.1. Cell culture and cell differentiation

Neural progenitor cell (NPCs) were generated as previously described [18]. Cells were scraped from the anterior portion of the lateral wall of the lateral ventricles of E14 embryonic mouse brains. The cells were grown as free-floating aggregates termed neurospheres. Dissociated cells were plated in DMEM/F-12 "complete" culture medium (Gibco) containing 2 mM L-glutamine, 15 mM HEPES, 100 U/ml penicillin, 100 μg/ml Streptomycin (all from Sigma-Aldrich), B27 supplement (Gibco), 20 ng/ml epidermal growth factor (EGF, PeproTech EC Ltd., London, UK), and 10 ng/ml basic fibroblast growth factor (bFGF, PeproTech EC Ltd., London, UK) and maintained in a humidified 5% CO_2/95% air incubator at 37 °C. Within 3–5 days the cells grew as free-floating neurospheres and were passaged after mechanical dissociation. For neuronal differentiation neurospheres were plated on poly-DL-ornithine (Sigma-Aldrich) coated culture plates in the absence of growth factors. Withdrawal of growth factors induces spontaneous migration of cells from the neurospheres and subsequent differentiation. The differentiated neural progenitor cells selected for pH and membrane potential measurements were single cells migrating towards the periphery, outside the neurosphere body. The total cell number in a typical neurosphere cluster varied between 300 and 1000 cells.

2.2. Materials

2′,7′-Bis(carboxyethyl)-5,6-carboxyfluorescein acetoxymethyl ester (BCECF-AM), pH-Rhodo AM, bis-(1,3-dibutylbarbituric acid)trimethine oxonol ($DiBAC_4(3)$), Rhod-2 AM and Fura-2 AM were from Invitrogen (Molecular Probes). All other chemicals used in the study were purchased from Sigma–Aldrich (Helsinki, Finland).

2.3. Solutions

The HEPES buffered medium (HBM) consisted of (in mM): 137 NaCl, 5 KCl, 2 $CaCl_2$, 0.44 KH_2PO_4, 4.2 $NaHCO_3$, 10 glucose, 10 HEPES, and 0.5 $MgCl_2$. The pH was adjusted to 7.35 with NaOH. Low K^+ medium contained 0.44 KH_2PO_4 (medium from which the KCL had been omitted). All experiments were performed at 37 °C under normal atmospheric conditions (21% O_2, 0.038% CO_2 in air).

2.4. Measurement of intracellular pH

Intracellular pH was measured in neural progenitor cells cell migrating outside the neurosphere by using the cell permeable probe 2′,7′-bis(carboxyethyl)-5,6-carboxyfluorescein acetoxymethyl ester (BCECF-AM) and a dual-wavelength InCytIm2 fluorescence imaging system (Intracellular Imaging Inc., Cincinnati, OH, USA). For the experiments, cells differentiated for 3 days on poly-ornithine coated 25 mm round coverslips were loaded with 4 μM BCECF-AM in HBM for 12 min at 37 °C. After the dye loading step, the cells were washed 3 times with HBM, placed in the measuring chamber and transferred to a temperature-controlled chamber holder on the microscope (Nikon, TMS, 20× objective). During the experiment, the cells were perfused (1 ml/min) with warm (37 °C) HBM pH 7.35. The cells were excited alternately with 490 and 440 wavelength light for 80 ms (rate of data capture 37 ratios/min). Rationed images from 100 single cells were analyzed with the Incyt 4.5 software and further processed with Origin 6.0 (OriginLab Corp., Northampton, MA) software. The BCECF fluorescence emission ratios (490/440) of the 510 nm fluorescence were turned into pH values by using a standard curve [10,19]. Briefly, single cells located outside the neurosphere body were equilibrated in K^+ medium (140 mM) of varying pH (5.0–8.5) in the presence of 5 μM nigericin and calibration curves were constructed by plotting the extracellular pH against the corresponding fluorescence ratio. A sigmoidal relationship between the 490/440-nm fluorescence ratio and pH was observed between pH 6.0 and 8.0.

2.5. Measurement of intracellular Ca^{2+}

Cells differentiated for 3 days on poly-ornithine coated 25 mm round coverslips were loaded with 2 μM Fura-2-AM (Invitrogen, Carlsbad, California, USA) in HBM for 15 min at 37 °C and subsequently transferred to a perfusion chamber. The imaging experiments were performed using an InCytIm2 fluorescence imaging system (Intracellular Imaging, Cincinnati, OH). The cells were perfused in HBM at 37 °C and excited by alternating wavelengths of 340 and 380 nm using narrow band excitation filters. Fluorescence was measured through a 430 nm dichroic mirror and a 510 nm barrier filter with a Cohu CCD camera. One rationed image was acquired per second and on-line ratio values were converted to $[Ca^{2+}]_i$ by using a calibration curve. The data collected from 100 single cells per experiment was analyzed with the InCyt 4.5 software and further processed with Origin 6.0 software (OriginLabCorp.).

2.6. Measurement of membrane potential

Changes in the resting membrane potential of mice neural progenitor cells differentiated for 3 days were monitored using the potentiometric bisoxonol dye bis-(1,3-dibutylbarbituric acid)trimethine oxonol ($DiBAC_4(3)$), an anionic probe that, exhibits enhanced fluorescence when the cell membrane is depolarized (increased intracellular fluorescence do to dye influx). Conversely, hyperpolarization of the membrane potential leads to efflux of the probe and a decrease in fluorescence intensity. Cells cultured on 25 mm round coverslips were washed 3 times with HBM pH 7.35, placed in the measuring chamber and transferred to the heat controlled chamber holder on the microscope (Nikon, Diaphot 200 inverted microscope, 20× objective). For the experiment, 500 nM $DiBAC_4(3)$ was added to the perfusion solution (HBM pH 7.35) and allowed to equilibrate across the cell membrane for 15 min (1 ml/min) before the data acquisition process was started. The cells were excited with 470 nm wavelength light for 80 ms (rate of data capture 30/min) and the emitted fluorescence captured at 530 nm. The data was collected and analyzed with the Till Vision software and further processed with Origin 6.0 (OriginLab Corp., Northampton, MA) software. At the end of each experiment, the cells were treated with depolarizing (20, 40 or 140 mM) K^+-solutions containing 500 nM $DiBAC_4(3)$ and the fluorescence signal was monitored. Membrane potential (E) was calculated using the Nernst equation assuming an intracellular potassium concentration of 140 mM and a temperature of 37 °C. $E = 2.303 \times RT/zF \times \log10\ ([K+]_e/[K+]_i)$. By using this system, $DiBAC_4(3)$ and Rhod-2 AM (dye loading with 1 μM for 12 min at 37 °C resulting in cytoplasmic dye loading) were also used to simultaneously record changes in membrane potential and intracellular calcium. For these measurements, we used a FITC/Cy3/Cy5 beam splitter (Chroma) to transmit the excitation lights to the sample while the emitted light from the cells was captured by using a green and red light transmitting filter.

2.7. Reverse Transcription – Polymerase Chain Reaction (RT-PCR)

Total RNA was isolated from mouse embryonic neural stem cells using RNAeasy Mini Kit (Qiagen). The RNA (2 μg) was reverse transcribed using Transcriptor High Fidelity cDNA Synthesis Kit (Roche).

Primers were adapted from Liu et al. [20].

NBCe1-SLC4A4	forward: 5-ACTTCTCTTGTGCTTGCCTGCC-3′ reverse: 5′-GATCCAGGTGATACCCAGCTCC-3′
NBCe2-SLC4A5	forward: 5′-GCCTCTGGATTGGTCTTCACTCAG-3′ reverse: 5′-CGGTTGACAATGACTGCGGTG-3′
NBCn1-SLC4A7	forward: 5′-GAGCCATCTAACCCTAGCAACG-3′ reverse: 5′-CATGAGCAAGTCAAGGTGGTAGC-3′
NDCBE-SLC4A8:	forward: 5′-GCTGGATGTCAAGCGGAAGG-3′ reverse: 5′-GACGATGAAGGTGGCGAAGAAC-3′

PCR: Initial denaturation 3 min at 95 °C, after which denaturation was performed for 30 s at 95 °C, annealing for 30 s at 55 °C, and elongation at 72 °C for 1 min (35 repeats). Negative controls included omission of cDNA. PCR products were separated by 110 V (40 min) by 2% agarose gel electrophoresis with ethidium bromide and photographed under ultraviolet illumination.

2.8. Immunocytochemistry

Cells differentiated for 3 days were fixed for 20 min at room temperature using 4% paraformaldehyde (Sigma) in phosphate-buffered saline (PBS, pH 7.4). Cells were permeabilized and blocked for unspecific staining with PBS containing 0.1% Triton X–100 and 1% bovine serum albumin (BSA) (all from Sigma), for 60 min at room temperature. Cells were then incubated with primary antibodies in PBS containing 0.1% Triton X–100 and 1% BSA overnight at 4 °C. Secondary antibodies were applied for 1 h at room temperature in the dark in 1% BSA-PBS. Primary antibody used to identify glia-like cells was guinea pig anti-Glutamate Transporter, Glial, IgG (GLAST) (AB1782, Millipore). The secondary antibody used was Alexa Fluor 568 goat anti-guinea pig IgG (A11075, Molecular Probes Invitrogen). The primary antibody used to stain migrating neurons was neuronal class III b-tubulin (TUJ 1), IgG (MMS-435P, Covance). The secondary antibody used was Alexa Fluor 488 donkey anti-mouse IgG (A21202, Molecular Probes, Invitrogen). Primary antibodies used to detect Na/HCO3 co transporters were rabbit polyclonal SLC4A4 and SLC4A8 (both from Abcam) and rabbit polyclonal SLC4A7 (Sigma). Secondary antibody used was Alexa Fluor 555 goat anti-rabbit IgG (Invitrogen). For secondary antibody controls, primary antibody was omitted, resulting in the disappearance of all staining. Cells were mounted using ProLong Diamond Antifade Mountant containing 4′,6-diaminodino-2-phenyl-indole (DAPI) for nuclear staining (Invitrogen) and viewed and photographed using an Olympus AX70 Provis microscope, 20× (numerical aperture 0.50) or 40× (numerical aperture 0.75) object magnification, equipped with a DP71 high resolution color digital camera (Olympus). A background reading was obtained from areas devoid of cells. This reading was reduced from fluorescence intensity values.

2.9. Neurosphere formation assay

NSCs spheres were dissociated by vigorous pipetting using a Pasteur pipette, centrifuged and re-cultured in DMEM/F-12 “complete” culture medium (Gibco) containing 2 mM L-glutamine, 15 mM HEPES, 100 U/ml penicillin, 100 µg/ml Streptomycin (all from Sigma-Aldrich), B27 supplement (Gibco), 20 ng/ml epidermal growth factor (EGF, PeproTech EC Ltd., London, UK), and 10 ng/ml basic fibroblast growth factor (bFGF, PeproTech EC Ltd., London, UK) and maintained in a humidified 5% CO_2/95% air incubator at 37 °C. For the assay, a suspension of single cells were plated in 24-well plates (2 ml/well) and incubated for 3 days. Neurospheres formed in the cultures were visualized and photographed by using an Axiovert 135 inverted microscope equipped with a Zeiss AxioCam HRm digital camera. The diameter of the neurospheres formed in the culture (indicative of proliferation potential) was measured by using the ImageG software.

2.10. Neuronal differentiation assay

For neuronal differentiation neurospheres were plated on poly-DL-ornithine- (Sigma) coated culture dishes in the absence of EGF and FGF. Growth factor withdrawal induced spontaneous neuronal differentiation. After 3 days, images were taken by using an Axiovert 135 inverted microscope equipped with a Zeiss AxioCam HRm digital camera (20× objective). The cell migration distance was measured by using the ImageJ software.

2.11. Statistics

Data are presented as means ± S.E.M. (n = number of cells, N = number of independent experiments). In each experiment 60–99 individual cells, located from the neurosphere body edge to the outer edge of the culture were randomly chosen. Each experimental condition was repeated at least three times with independent neural progenitor cell preparations. In all experiments, pH_i was allowed to decline for 4 min followed by calcium removal to initiate the pH recovery phase. The pH decline or recovery rate is given as ΔpH/min. Student's unpaired *t*-test was used to compare differences between the two cell populations.

3. Results

3.1. Characterization of the cell-populations present in the differentiated neurosphere culture

In our previous published work, we have shown that two distinct main populations of cells coexist among the migrating cells [10,21]. A typical neurosphere culture differentiated for 3 days, stained with DAPI, GLAST and Tuj 1 antibodies is shown in Fig. 1.

In the overlaying image (Fig. 1C), an inner layer of GLAST stained radial glia-like cells and an outer Tuj 1 neuronal marker positive layer with migrating neurons can be seen. To functionally identify these cell population we studied intracellular calcium signaling in Fura 2 loaded cells by using (*S*)-3,5-dihydroxyphenylglycine (DHPG), a potent agonist of group I metabotropic glutamate receptors (mGluRs) and Kainate as ligands [22]. The inner GLAST positive cell population (located closer to the sphere edge) responded to DHPG, an agonist of metabotropic glutamate receptor 5 (mGluR5) expressed in the radial glial population [21], but not to the AMPA/kainate receptor agonist, Kainate (Fig. 1E). The outer Tuj 1 positive cell population responded only to Kainate and was mostly found in the periphery of the sphere culture (migrating neurons) (Fig. 1F).

3.2. The majority of the DHPG responsive cells are acidified by low extracellular potassium

We have previously shown that hypoxia causes hyperpolarization and acidification of the radial glial-like cell population [10]. The membrane potential of the radial glial-like cells is dependent on extracellular K^+ and thus reduction in extracellular K^+ triggers hyperpolarization. To study the functional properties of the radial glia-like cells that responded to DHPG we next performed intracellular calcium and pH measurements (Fura-2 and BCECF) on the same cell population. Measurement of pH_i indicated that the majority of cells that responded to DHPG in our Fura-2 experiments (49.2% of the whole cell population) were also acidified upon exposure to low extracellular K^+. Typical Fura-2 and BCECF traces of two individual cells, here named cell 1 and cell 2, are shown in Fig. 2A and B. By performing this type of combined measurements, we found that 82.4% ± 5.8% of the cells that responded to DHPG were also acidified by low K^+ treatment. Only 13.7% ± 0.9% of the cells that did not respond to DHPG were acidified.

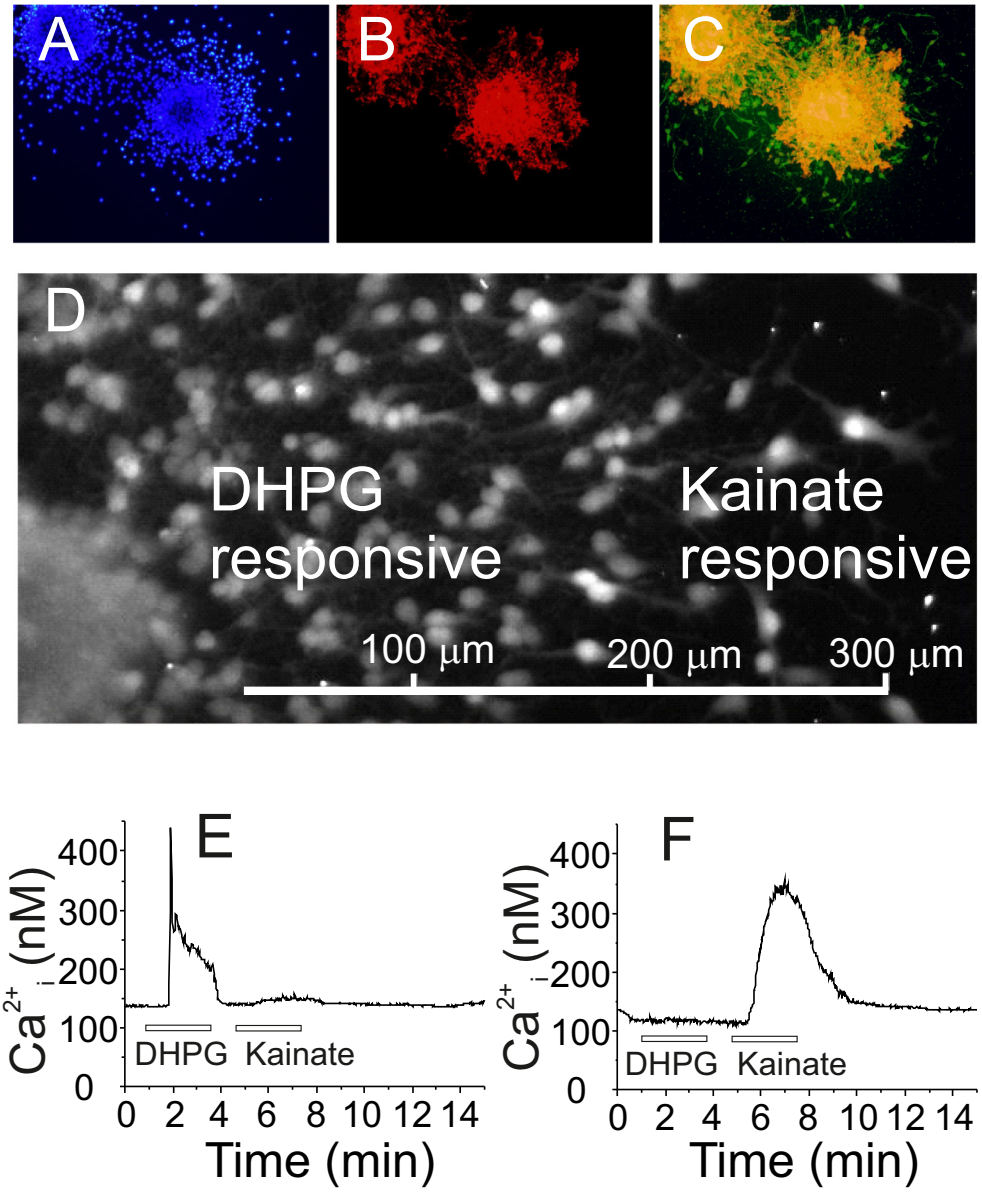

Fig. 1. Cell populations present in a differentiated embryonic neurosphere culture. Immunostaining on a neurosphere culture differentiated for 3 days. (A) DAPI, (B) GLAST and (C) overlay images of Tuj 1 and GLAST staining. (D) Image of BCECF loaded cells showing the location of the main DHPG and Kainate responsive cells. (E). Typical DHPG (10 μM) induced Ca^{2+} response in a Fura-2 loaded inner cell and an outer cell responsive to Kainate (50 μM) (F).

3.3. Hyperpolarization-induced sustained acidification in the inner cell population is dependent on extracellular calcium

By using BCECF as an intracellular pH indicator we found that the two populations of cells (inner radial glia-like cells and outer cells consisting mostly of migrating neurons) could clearly be distinguished based on their intracellular pH response to low extracellular potassium-induced hyperpolarization. A typical response of the inner cell population is shown in Fig. 3A.

When cells were exposed to low extracellular K^+ in the presence of 2 mM extracellular calcium intracellular acidification took place. Upon removal of extracellular calcium a rapid recovery in intracellular pH occurred. On the other hand, in the absence of extracellular calcium a transient acidification could be seen in the inner cell population (Fig. 3B). Lowering the extracellular calcium concentration from 2 mM to 1 mM, already allowed pH recovery in 20% of the acidified cells. When the extracellular calcium concentration was further lowered, down to 0.5 mM, extensive pH_i recovery could be observed in 38.5% of the acidified glial-like cell population.

By using $DiBAC_4(3)$-equilibrated cells, to measure membrane potential, we observed that cells perfused with modified HBM pH 7.35 containing 0.44 mM K^+ induced a 10 mV hyperpolarization in the inner radial glia-like cell population (Fig. 3C). However, removal of all extracellular Ca^{2+} initiated a prompt depolarization in the cell population. A depolarization that was 10 mV or higher than the initial resting membrane potential could be observed in 39.2% ± 5%, (N = 6) of the whole cell population. In the rest of the cells, a smaller hyperpolarization of 6.6 mV ± 0.3 mV could be observed. When the cell population was perfused with calcium free 0.44 K^+ solution, the membrane potential returned to its original value (no overshoot observed). In our experiments conducted in modified medium, where all Na^+ was isoosmotically replaced with NMDG+ (*N*-methyl-D-glucamine), no depolarization or pH recovery could be observed after Ca^{2+} removal (data not shown). This strongly indicated that Na^+ influx was responsible for the depolarization observed.

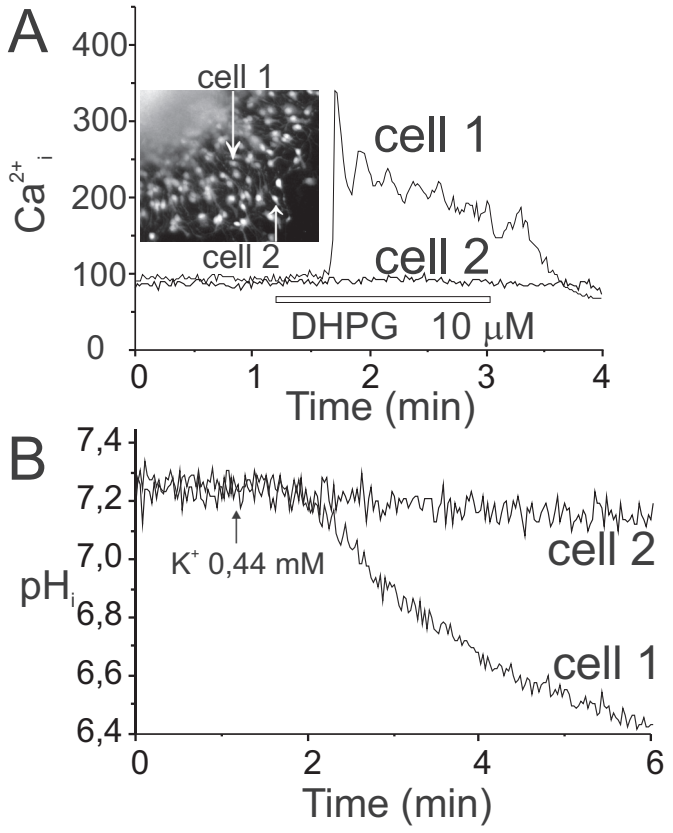

Fig. 2. The cell population that is acidified by low potassium is DHPG responsive. (A). Location of cell 1 and cell 2 and intracellular Ca^{2+} response upon exposure to 10 μM (*S*)-3,5-dihydroxyphenylglycine (DHPG). (B). Subsequent BCECF loading and intracellular pH signal in the same cells exposed to low extracellular potassium (modified HBM containing 0.44 mM K^+).

3.4. Depolarization with high extracellular potassium overrides the inhibitory effect of extracellular calcium on the pH recovery phase

Having found that Ca^{2+} apparently interferes with a Na^+ channel that mediates the depolarization we next studied whether pH recovery take place in hyperpolarized and acidified cells when they are exposed to high extracellular potassium. As shown in Fig. 4A, a rapid recovery in cytosolic pH took place when 20 mM K^+ was added.

This recovery was evident in 27.3% ± 2.4% of the whole cell population. In the rest of the cells, mostly consisting of migrating neurons, a very modest low K^+-induced acidification and response to 20 mM K^+ could be observed (Fig. 4B). Perfusion with 20 mM K^+ induced a prompt depolarization in the hyperpolarized cells despite the fact that 2 mM extracellular Ca^{2+} was present.

3.5. Low extracellular potassium induces hyperpolarization and elevation in cytosolic calcium in radial glia-like cells

To study whether intracellular calcium is changed during the treatment with low K^+ we next performed multichannel experiment where we simultaneously measured intracellular pH and Ca^{2+}. As shown in Fig. 5A, lowering extracellular K^+ induced a rapid increase in intracellular calcium in Rhod 2 loaded cells. When extracellular calcium was removed, intracellular pH recovered and intracellular Ca^{2+} declined. Subsequent perfusion with 10 mM NH_4Cl in HBM containing 2 mM Ca^{2+}, that induces pH_i increase and washout that causes strong intracellular acidification, did not cause changes in intracellular Ca^{2+}.

By performing multichannel fluorescence excitation on Rhod-2-loaded and $DiBAC_4(3)$-equilibrated cells, we found that the inner cell population responded to low extracellular K^+ by giving a simultaneous increase in Rhod-2 fluorescence (calcium influx) and decrease in $DiBAC_4(3)$ fluorescence (hyperpolarization), (Fig. 5B). The outer cell population showed a much weaker responses, (Fig. 5C).

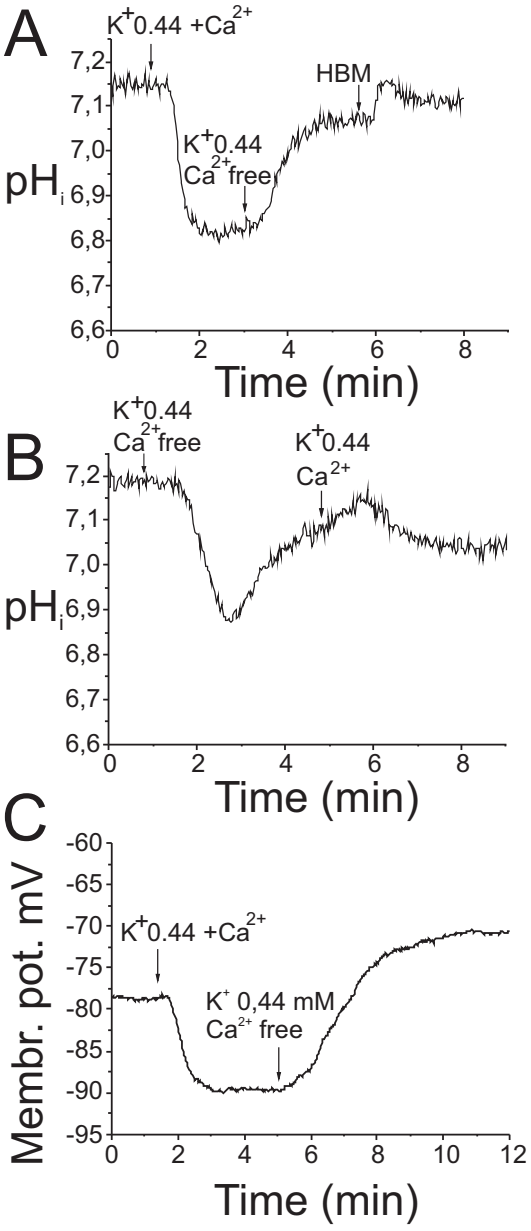

Fig. 3. Effects of extracellular calcium on low K+ induced intracellular acidification and hyperpolarization in glia-like cells. (A). Intracellular pH response in inner radial-glia like cells exposed to low extracellular K^+ in the presence of 2 mM extracellular calcium. Removal of calcium induced a recovery in intracellular pH. (B) Intracellular pH response in inner radial-glia like cells exposed to low extracellular K^+ in the absence of extracellular calcium. A transient acidification is seen. (C). Change in membrane potential in $DiBAC_4(3)$ equilibrated glia-like cells upon exposure to low extracellular K+. Low 0.44 mM K^+ induced a hyperpolarization while a prompt depolarization occurred after removal of extracellular calcium. In every individual experiment, a pH response from 100 cells was recorded. Representative traces (average) of the inner glia-like cell population are shown.

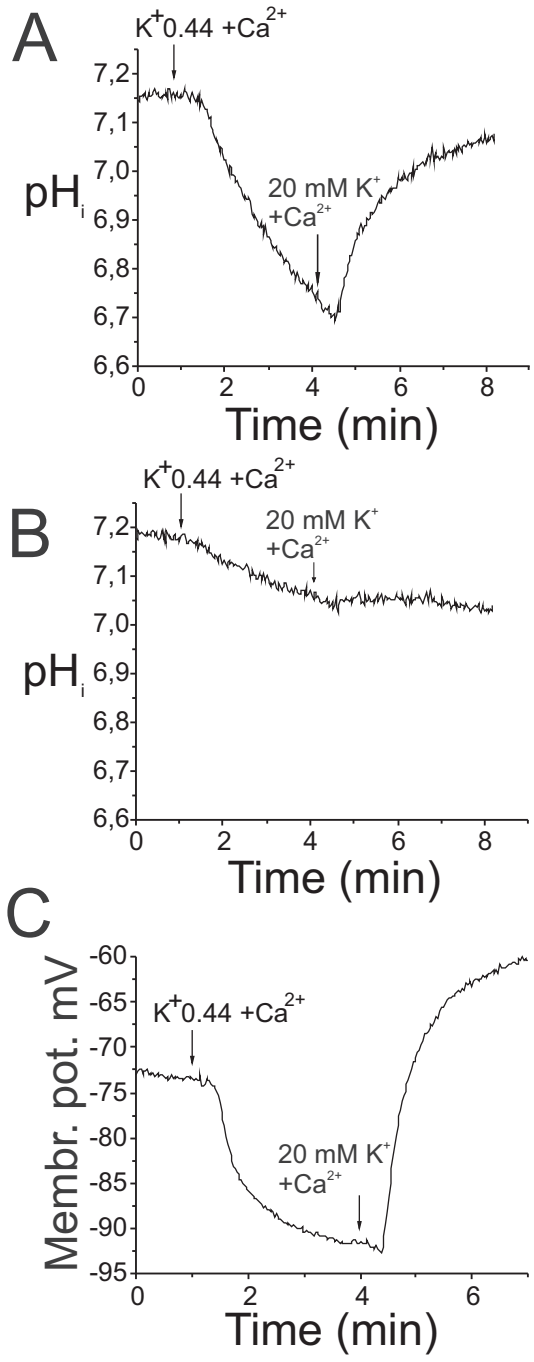

Fig. 4. Intracellular pH recovery and changes in membrane potential induced by high extracellular K^+ in glia-like cells. (A). Intracellular pH response in inner radial-glia like cells exposed to low extracellular K^+ in the presence of 2 mM extracellular calcium. Addition of 20 mM K+ induced a recovery in intracellular pH. (B) Intracellular pH response in the outer neuronal like cells exposed to low extracellular K^+ followed by high 20 mM extracellular K^+. (C) Change in membrane potential in $DiBAC_4(3)$ equilibrated glia-like cells upon exposure to low extracellular K+ (0.44 mM K^+) and 20 mM K^+. In every individual experiment, a pH response from 100 cells was recorded. Representative traces (average) are shown. N = 3.

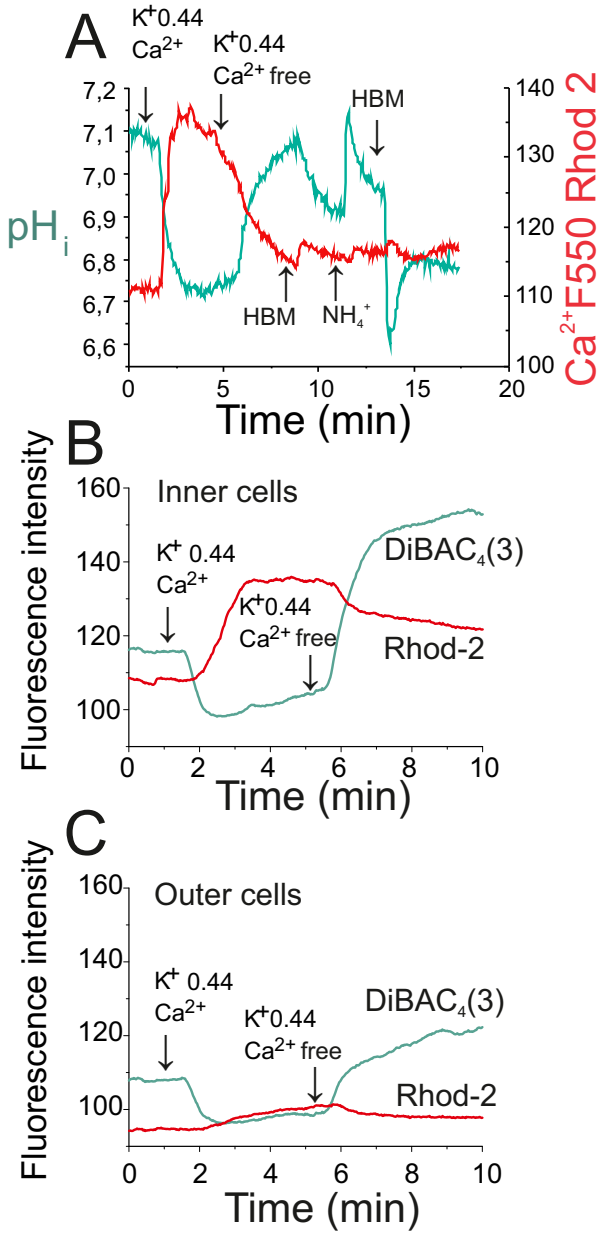

Fig. 5. Effects of low potassium on intracellular Ca^{2+} in neural progenitor cells. (A). Change in intracellular pH and calcium in neural progenitor cells exposed to modified HBM (pH 7.35) containing 0.44 mM K^+ and 2 mM Ca^{2+}, calcium free HBM (pH 7.35) containing 0.44 mM K^+ or HBM (pH 7.35) containing 10 mM NH_4^+ (followed by washout of NH_4^+). (B). Change in intracellular calcium (increase in Rhod-2 fluorescence indicates increase in intracellular calcium) and membrane potential (decrease in $DiBAC_4(3)$ fluorescence indicates hyperpolarization) in radial glia-like cells (inner cells) exposed to Ca^{2+} containing modified HBM (pH 7.35) with 0.44 mM K^+. (C). Change in Rhod-2 fluorescence and $DiBAC_4(3)$ fluorescence in migrating neurons (outer cells) exposed to Ca^{2+} containing modified HBM (pH 7.35) with 0.44 mM K^+. Results from cells differentiated for 3 days are shown. In every individual experiment, a response from 100 cells was recorded. Representative traces (average) of the inner and outer cell populations are shown.

3.6. Rapid recovery in pH_i after calcium removal requires extracellular bicarbonate and can be prevented by a potent NBC inhibitor S0859

In order to trace the origin of the protons (acid equivalents) that induced intracellular acidification in cells exposed to low extracellular K^+, we performed experiments in nominally bicarbonate-free salt solutions. As shown in Fig. 6A, when cells were loaded with BCECF in HCO_3^- free HBM for 10 min, low K^+ and HCO_3^--free solution induced only a modest intracellular acidification in the inner cell population. In addition, under HCO_3^- free conditions, subsequent removal of calcium did not trigger pH_i recovery. Likewise, perfusion with bicarbonate-free HBM did not cause pH recovery while perfusion with bicarbonate

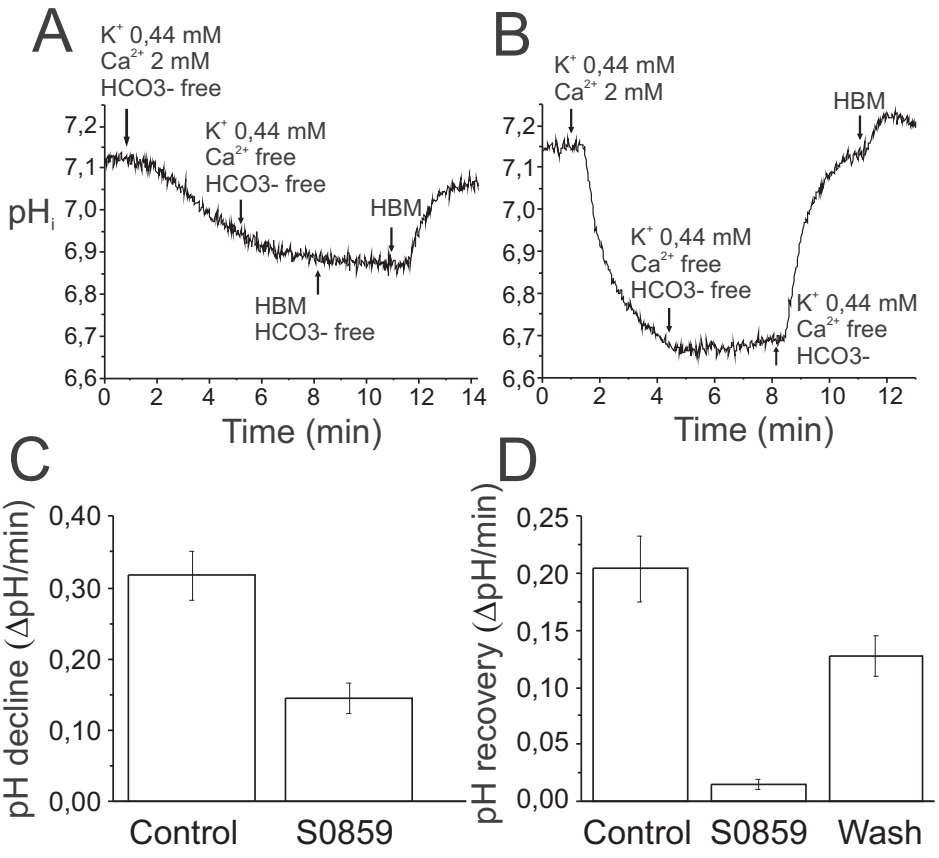

Fig. 6. Effects of extracellular bicarbonate and S0859 on low potassium induced intracellular acidification and pH recovery after calcium removal. (A). Change in intracellular pH in neural progenitor cells loaded with BCECF in the absence of bicarbonate followed by exposure to modified bicarbonate free HBM medium containing 0.44 mM K^+ (B). Acidification in cells perfused with HBM containing 0.44 mM K^+ and 2 mM Ca^{2+}. Effect Ca^{2+} removal in the absence and presence of bicarbonate. (C). Effect of 25 μM S0859 on low K^+-induced and bicarbonate-dependent acidification and pH recovery after Ca^{2+} removal (D). pH-decline- and pH-recovery rates are given as mean ΔpH/min ± SEM (N = 5, results of 100 cells in each experiment). Representative traces (average of 100 cells in each experiment) of inner cells differentiated for 3 days are shown.

containing HBM induced a prompt recovery in pH_i. As shown in Fig. 6B, very modest recovery in pH_i took place when cells, acidified by low K^+ in the presence of Ca^{2+} and $HCO3^-$,were perfused with calcium-free and HCO_3^- free 0.44 mM K^+ solution. Subsequent perfusion of the cells with calcium-free 0.44 mM K^+ solution containing 4.2 mM HCO_3^- induced an instant recovery in intracellular pH (Fig. 6B).

Intracellular pH regulation and pH recovery from an intracellular acid load has previously mainly been studied by using the ammonium pre-pulse technique. However, in our system we induce intracellular acidosis in glial cells by exposing them to hyperpolarizing low K^+ medium that drives out $HCO3^-$ from the cell leaving protons behind. To evaluate which pH regulatory mechanism is responsible for the pH_i recovery process, observed here after calcium removal, we used S0859, an *N*-cyanosulphonamide compound that inhibits NBCs [23]. S0859 only marginally altered cytoplasmic pH under basal conditions. The pH_i was 7.22 ± 0.02 before the addition of 25 μM S0859 and 7.24 ± 0.01 (N = 3) after this addition. When pH_i was measured in low K^+-exposed radial glial-like cells in the presence of 25 μM S0859, the acidification rate was 44% slower (pH decline rate was 0.14 ± 0.02 pH/min as compared to 0.32 ± 0.03 pH/min in control cells) (Fig. 6C). On the contrary, the pH_i recovery phase after calcium removal was strongly inhibited (Fig. 6D). In the presence of 25 μM S0859 the pH recovery rate was 0.015 ± 0.004 pH/min as compared to 0.20 ± 0.03 pH/min in control cells. The inhibition was reversible since washout of S0859 resulted in prompt recovery in pH_i (0.13 ± 0.02 pH/min).

3.7. Electrogenic (SLC4A4) and the non-electrogenic (SLC4A7) sodium/bicarbonate cotransporters are expressed in the stem cell glia-like cell population

Since S0859, inhibited the pH_i recovery from acidosis, we assumed that one type of the sodium driven chloride bicarbonate exchanger (NDCBE) or sodium bicarbonate cotransporters (NBC) operate in the radial glia-like cell population. Immunostaining with antibodies showed that SLC4A4 (NBCe1) and SlC4A7 (NBCn1) are expressed in the differentiated cell population (Fig. 7A, B and C) Especially, SLC4A4 showed strong expression in the radial glia layer (radial processes) (Fig. 7A and B). The electroneutral transporter SLC4A7 (NBCn1) showed much weaker immunostaining (Fig. 7C) while no positive SLC4A8 (NDCBE) staining could be observed (data not shown). To verify this, we also run RT-PCR on our cell population that has been differentiated for 3 days. Our RT-PCR data showed that SLC4A4 (NBCe1), SlC4A7 (NBCn1) were present while low expression of SlC4A8 (NDCBE) mRNA was present in the cell population. SLC4A5 was not expressed (Fig. 7D).

3.8. Sodium/bicarbonate cotransporters (NBCs) are important for asymmetric cell division of radial glia-like progenitor cells that generates radial glial cells and migrating neurons

Removal of the growth factors EGF and FGF from neurospheres cultures plated on poly-DL-ornithine coated coverslips results in cell differentiation giving radial glial cells and migrating neurons [22]. To study the impact of NBC inhibition on the cell differentiation process, we differentiated neural stem cells in the presence of the NBC inhibitor S0859. As shown in Fig. 8C, cell differentiation (for 3 days) was strongly inhibited by 25 μM S0859 as compared to control (Fig. 8A) and DMSO-treated (Fig. 8B) cell cultures.

In the culture treated with S0859, reduced amounts of migrating neurons were present and the migrating distance was shorter (Fig. 8C and G). Likewise, the NBC inhibitor S0859, had a strong impact on the neurosphere formation (stem cell proliferation) in the presence of EGF and FGF. In the presence of 25 μM S0859, formation of large neurospheres was inhibited (sphere diameter 69.6 ± 2.0 μm versus 184.0 ± 5.6 μm in control cultures) and single cells forming a connection network appeared in the cell culture (Fig. 8D, E and F).

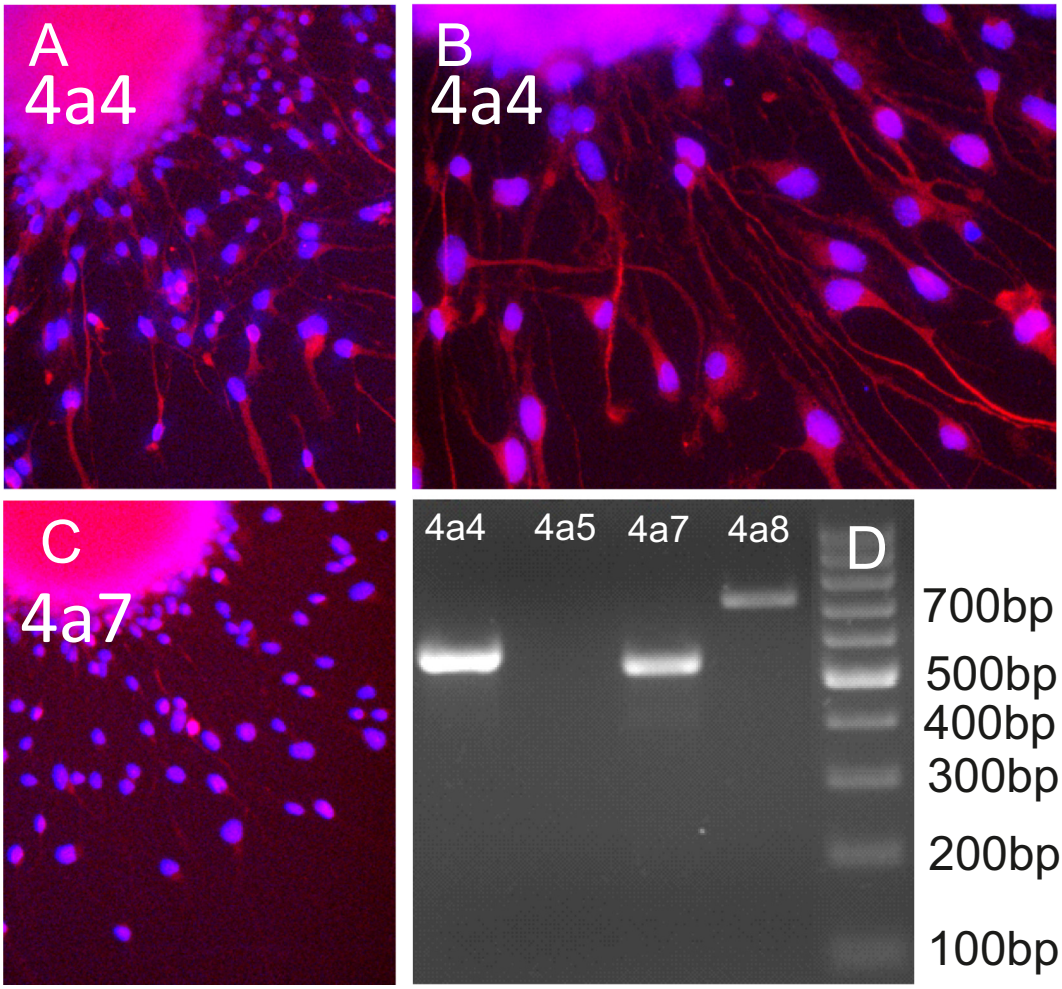

Fig. 7. Expression of bicarbonate transporters in neural progenitor cells. Overlay of immuno- and DAPI staining showing expression of (A) NBCe1 (SLC4A4) (C) NBCn1 (SLC4A7) in neural stem cells differentiated for 3 days. (B) Higher magnification of cells immunostained with antibodies to SLC4A4 (overlay with DAPI) showing strong reactivity in glial cells and glial processes. (D) Gene expression of mRNA of various members of SLC4 family extracted from neural progenitor cells by RT-PCR. Lane 1, NBCe1 (SLC4A4), lane 2, NBCe2 (SLC4A5), lane 3, NBCn1 (SLC4A7) and lane 4, NDCBE (SLC4A8).

3.9. The S0859 induced cell network in the stem cell culture consists of functionally competent neurons and radial glia-like cells

The network forming cells that appeared in the cell culture in the presence of S0859 was further characterized by immunostaining together with functional studies using glutamate receptor ligands and calcium imaging. As shown in Fig. 9, panel A, the cell clusters stained positive for the glial marker GLAST while very bright immunostaining of TUJ-1 could be observed in some neurons. A population that was stained by both markers was also present in the cell culture (Fig. 9B). To evaluate whether these migrating cells where functional, we next performed calcium imaging experiments on the whole cell population. Among the cells, we found a small population of cells that responded only to Kainate, a ligand that mainly stimulate ionotropic glutamate receptors in neurons (Fig. 9C). However, two major populations responding only to DHPG or both ligands were abundant. An immature cell population that did not respond to these stimuli was also present (Fig. 9D).

4. Discussion

Undifferentiated neural stem cells have the potential to differentiate and give rise to various specialized cell types such as radial glial cells, neurons and oligodendrocytes. After an acute brain lesion, such as trauma and stroke, stem cells migrate from the subventricular zone, a region where new stem cells are formed, to the site of injury [4,24]. However, it is still unclear how the signaling molecules released from the injured site together with local alterations in the oxygen level and ionic composition due to brain oedema (e.g. Ca^{2+}, K^{+}), trigger the neural stem cell proliferation, differentiation and migration process.

A well-documented physiologic alteration in the microenvironment at the site of a brain injury is hypoxia and acidosis [25–27]. This does not only concern stroke in elderly, but intrauterine hypoxia during pregnancy may also play a significant role in early brain development and mental development later in life [28]. Hypoxia causes alterations in the extracellular ionic environment. Typically an increase in extracellular K^{+} concentrations and lowering of extracellular Ca^{2+} is seen but sporadic reports can be found in the literature describing severe or moderate hypokalemia in (TBI) patients [29–32]. Thus, local alterations in K^{+}, or hypoxic environment that causes membrane hyperpolarization, might affect various voltage-dependent ion transport systems in cells, including stem cells invading the injured area.

We have previously shown that hypoxia causes hyperpolarization and acidification of radial glial cells, which function as a scaffold for migrating neurons [10]. In this study, we have used differentiated mouse embryonic stem cells as our model system to study the effects of extracellular K^{+} on pH_i. To identify the cells in this population, we performed functional studies using Kainate and DHPG. DHPG is a ligand that triggers calcium signaling by activating metabotropic glutamate receptor 5 (mGluR5) receptors in the glial glutamate-aspartate

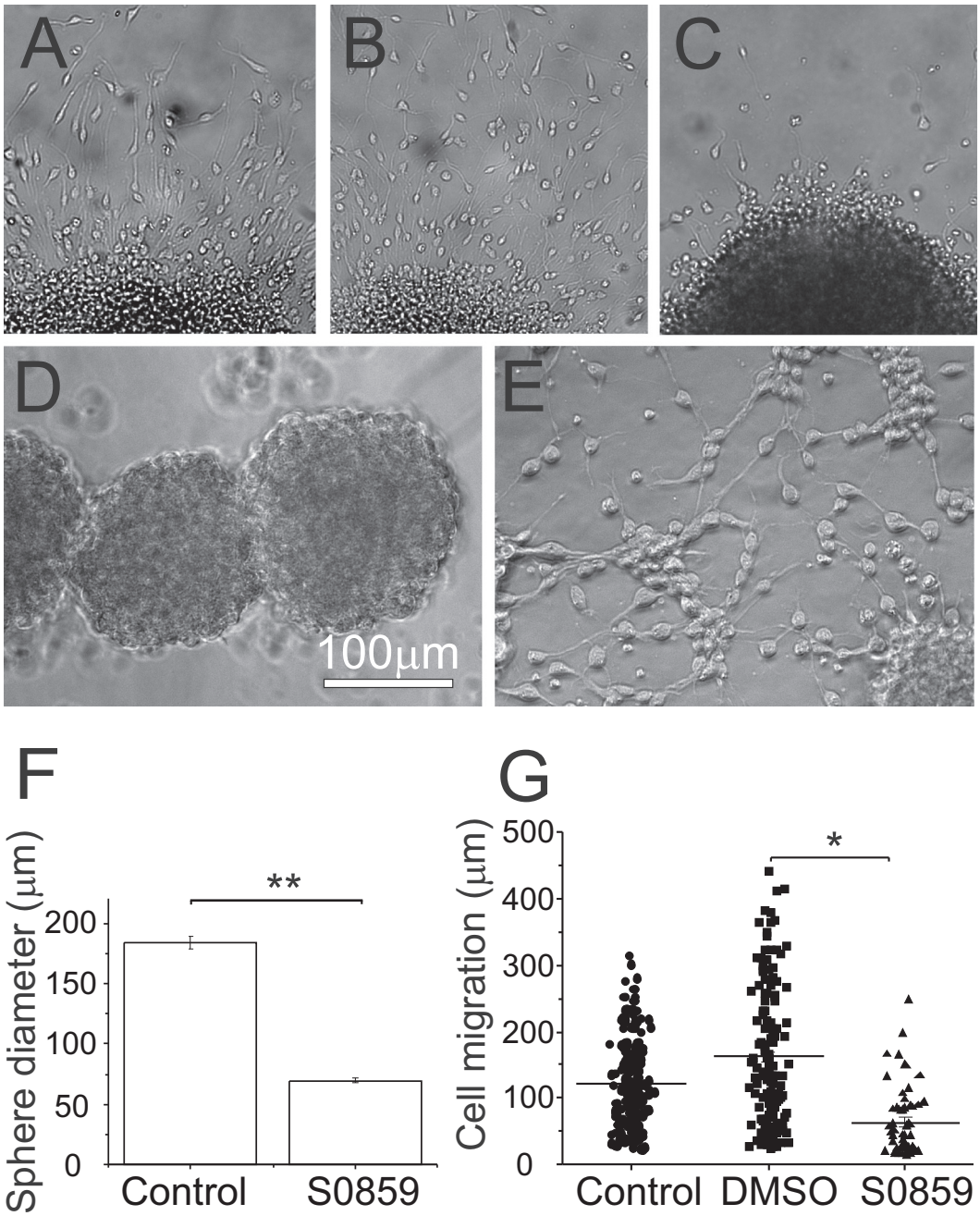

Fig. 8. Inhibition of Sodium/bicarbonate cotransporters (NBCs) affects neural stem cell differentiation and proliferation. Images showing cell differentiation patterns (on day 3) of (A) control, (B) DMSO or (C) 25 µM S0859-treated cultures. (D) Image of a typical neurospheres formed within 72 h in control culture or (E) cultures treated with 25 µM S0859 in normal growth medium DMEM/F12 supplemented with B27, glutamine, Hepes, FGF and EGF. (F) Neurosphere size (diameter in µm) in control and S0859 treated cultures. Data are presented as means ± SEM from three independent experiments, (50 spheres measured in each group) (**$p < 0.01$). (G) Cell migration distance (µm) in culture differentiated for 72 h. Horizontal lines indicate means. The means are significantly different (*$p < 0.05$).

transporter (GLAST)-positive cell population [21,33–35]. By performing calcium and pH measurements on the same cell population we found that a majority of the cells that responded to DHPG by giving a calcium signal were also acidified upon exposure to low K^+ medium. This indicates that the radial glia-like cells are the main cell population that is acidified during hypokalemic conditions.

Interestingly, we found that the sustained intracellular acidification caused by low extracellular K^+ was highly dependent on extracellular calcium. Removal of extracellular calcium caused a rapid pH recovery in hyperpolarized cells that had been kept acidic in the presence of extracellular calcium. During calcium free conditions, reduced extracellular K^+ levels induced only a transient acidification. Thus, local extracellular calcium concentration can have a strong impact on hypoxia-induced hyperpolarization and acute intracellular acidification. Instant pH_i recovery could already be observed in some individual radial glial cells when extracellular calcium was lowered from 2 mM to 1 mM. The blocking effect of extracellular Ca^{2+} was indicative of a channel block, probably on a Na^+ permeable channel, that is responsible for the observed rapid depolarization (Na^+ influx). Lowering, or complete removal of extracellular calcium, has earlier been reported to activate sodium permeable "leak channels" [36,37]. Nonselective Na^+ and Ca^{2+} permeable TRPC channels are expressed in our neural stem cells [34] and would be a likely candidate for the effects seen. However, several other channels of this type exist, so the identity of the

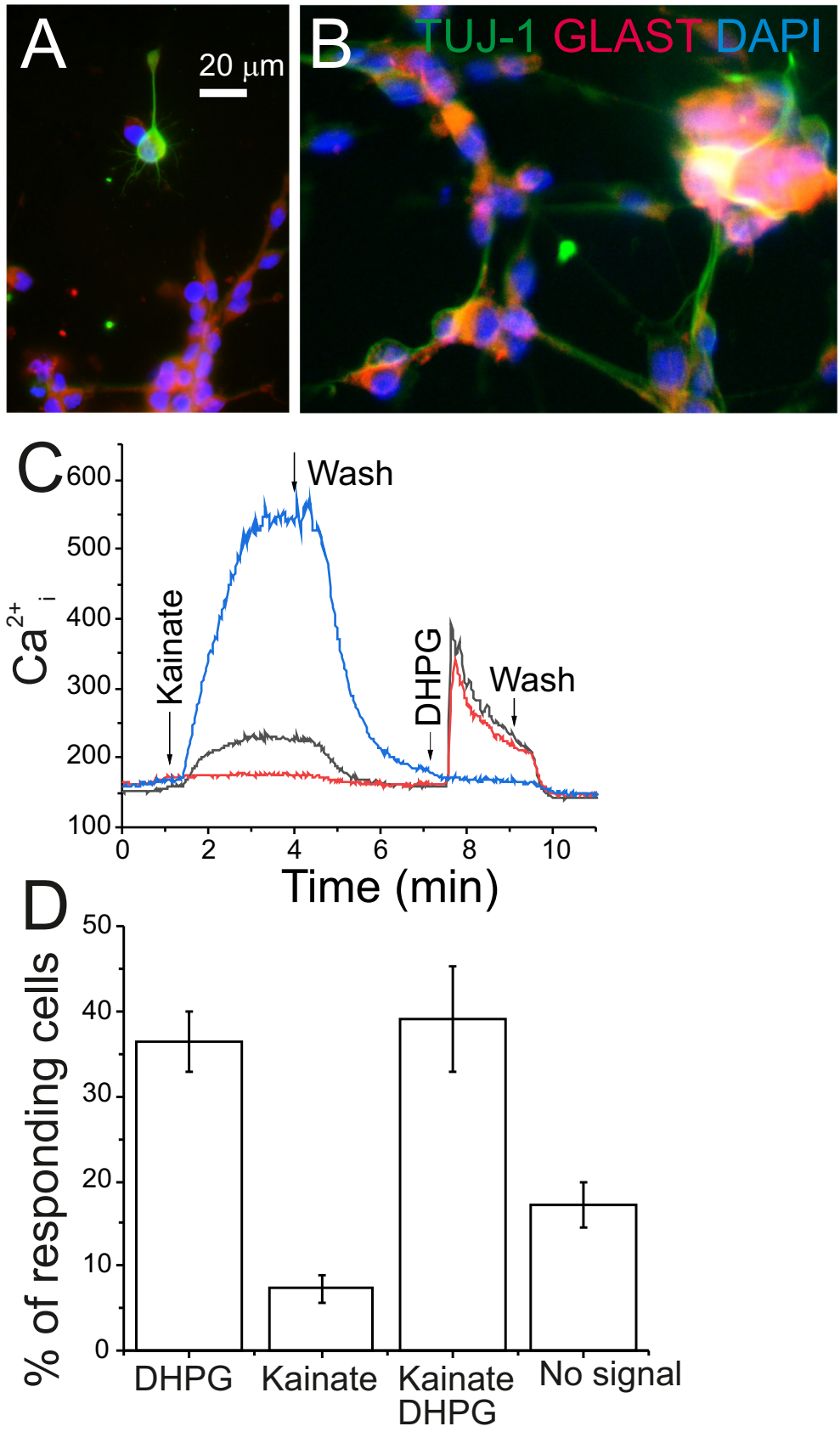

Fig. 9. Characterization of cells formed by S0859 in a proliferating neural stem cell culture. (A and B) Overlay TUJ-1 and GLAST immuno- and DAPI staining of neural progenitor cells cultured for 3 days in the presence of 25 μM S0859. (C) Kainate (50 μM) and DHPG (10 μM) induced Ca^{2+} responses in Fura-2 loaded cells cultured in the presence of 25 μM S0859 for 3 days. (D) Graph showing the % of cells responding to Kainate, DHPG or both stimulus. In (C) representative traces (average of 100 cells in each experiment) of the whole cell population are shown. Results in (D) are mean ± SEM (N = 3, results of 100 cells in each experiment).

Na^+ channel involved remains to be studied.

Our findings are relevant since it has earlier been reported that the calcium concentration in the cerebrospinal fluid decreases in TBI from 1 to 0.01 mM [38,39]. During such conditions, NBCs might be active and keep glial cell pH_i alkaline in a hypoxic environment. Depolarization and intracellular alkalinization, stimulates exocytotic and non-vesicular glutamate release from glial cells, causing neuronal cytotoxicity [40–43].

Lowering extracellular K^+ induced intracellular acidification and a rapid increase in intracellular calcium. However, treatment with NH_4Cl and washout, a method used to induce rapid intracellular alkalinization and acidification in cells, did not cause changes in intracellular Ca^{2+}. This indicates that intracellular acidification per se is not responsible for the calcium signal seen. More likely, hyperpolarization increases the driving force for Ca^{2+} fluxes into these cells.

In neuronal cells, acute hypoxia is known to trigger hyperpolarization caused by activation of ATP-sensitive K^+ (K_{ATP}) channels [44] or activation of calcium dependent K^+ (K_{Ca}) channels [45]. We found that low K^+ induced a prompt hyperpolarization in the whole stem cell population and lowered the resting pH_i in the DHPG responsive glia-like cell population. From an electrophysiological point of view, hyperpolarization tends to increase the driving force for cation influx e.g. protons (H^+) and extrusion of anions such as bicarbonate ($HCO3^-$) and hydroxyl ions (OH^-) (base efflux). Since we found that the low extracellular K^+-induced acidification was highly dependent on the presence of a bicarbonate buffer system, we concluded that the acidification and proton generation is most likely due to rapid bicarbonate extrusion (leaving protons behind). Extracellular bicarbonate apparently increases the intracellular free HCO_3^--pool that electrogenically can rapidly be extruded from cells during hyperpolarized conditions. Likewise, we found that the rapid pH recovery process after calcium removal is dependent on a bicarbonate buffer system that can support a bicarbonate influx.

Our finding that the pH recovery after calcium removal, in glia-like cells acidified by low extracellular K^+, was inhibited by the NBC inhibitor S0859 further strengthen the view that a bicarbonate-dependent transporter is involved in the pH_i recovery process (Fig. 6C and D). Several types of Cl/HCO3 exchangers, sodium driven chloride bicarbonate exchanger (NDCBE) or sodium bicarbonate co-transporters (NBC) has been discovered in various cell types [46]. Electrogenic Na/HCO3 cotransporter has been found in glial cells and the electroneutral Na/HCO3 cotransporter NBCn1 has earlier been described in rat hippocampal neurons [47–49]. NDCBE has been shown to be present in human, mice and rat brain tissue [50,51] and to participate in pH regulation in rat neurons, astrocytes and glial cells [52–54].

Extracellular HCO_3^- was important for the pH recovery process and therefore any of the NBCs (SLC4A4; NBCe1, SLC4A5; NBCe2, SLC4A7; NBCn1) or Na^+ driven HCO_3^- transporters e.g. NDCBE (SlC4A8) could be involved in the process. Our findings with, immunostainings and PCR indicated that the pH recovery process in hyperpolarized radial glial cells is mainly mediated by the electrogenic NBCe1 (SLC4A4) that was activated when the extracellular calcium was removed. Upon removal of calcium, the radial glial cell membrane potential was rapidly depolarized that triggered $Na+:nHCO3-$ influx (complex with negative charge). Immunostaining experiments showed that NBCe1 (SLC4A4) was highly expressed in radial glial processes. However, in a fraction of cells NBCn1 (SLC4A7) was apparently operative since pH recovery took place in some cells where no rapid depolarization could be observed.

Based on our findings, it became apparent that radial glia-like neural stem cells mostly rely on NBC systems and not Na/H antiporters to regulate intracellular pH during acute hypoxia. This could clearly be seen in our experiments with stem cell differentiation and proliferation where we used S0859. Thus, we provide, for the first time, experimental evidence demonstrating that sodium/bicarbonate cotransporters (NBCs) are important for production of neurons and radial glial cells. Moreover, we show that proliferating neuronal stem cells/progenitor cells that grow in clusters, rely on functional NBCs to neutralize the acid load generated in the neurosphere. When this pH_i regulating system was inhibited, cells could not form large (100–200 μm in diameter) neurospheres but instead aggregated in smaller neurosphere clusters with a special single cell network. Our immunostainings and Ca^{2+} imaging experiments clearly indicated, that these cells building a network in the presence of the NBC inhibitor S0859, are glia-like cells and neurons that are functionally competent. These findings are in line with studies of glioma cells (whose origin is thought to be from radial glia) where hypoxia has been shown to induce SLC4A4 expression. Accordingly, knockdown of SLC4A4 expression inhibits cell proliferation [55]. Since hypoxia-stimulated neurogenesis is also mediated by hypoxia-inducible factors (HIFs) [56], it is tempting to suggest that the Na/HCO3 cotransporter SLC4A4 is part of the neurogenesis program protecting progenitor cells from acidosis. We have previously shown that progenitor cells are very resistant to a low pH environment [10].

In summary, by exposing differentiated neural stem cells to low K^+, we demonstrate that radial glia-like cells are rapidly hyperpolarized and acidified due to electrogenic $HCO3^-$ efflux. Our results demonstrate that calcium signaling is linked to $HCO3^-$-dependent pH regulation in glia-like progenitor cells. Our data provide new insights into the mechanism by which calcium plays a key role in glial/neuronal communication during ischemic conditions. Our results, showing effects of calcium on membrane potential and intracellular pH regulation, are relevant when it comes to ischemia/reperfusion injury in brain tissue [57,58].

Transparency document

The Transparency document associated with this article can be found, in online version.

Acknowledgments

Supported by grants from the K. Albin Johansson foundation, the Magnus Ehrnrooth foundation, Medical Society of Finland and The Swedish Cultural Foundation in Finland. We are grateful for the laboratory assistance provided by Jarno Hörhä and Linda C Jansson.

References

[1] F.R. Sharp, J. Liu, R. Bernabeu, Neurogenesis following brain ischemia, Brain Res. Dev. Brain Res. 134 (2002) 23–30.
[2] L.L. Zhu, T. Zhao, H.S. Li, H. Zhao, L.Y. Wu, A.S. Ding, W.H. Fan, M. Fan, Neurogenesis in the adult rat brain after intermittent hypoxia, Brain Res. 1055 (2005) 1–6.
[3] X.H. Zhu, H.C. Yan, J. Zhang, H.D. Qu, X.S. Qiu, L. Chen, S.J. Li, X. Cao, J.C. Bean, L.H. Chen, X.H. Qin, J.H. Liu, X.C. Bai, L. Mei, T.M. Gao, Intermittent hypoxia promotes hippocampal neurogenesis and produces antidepressant-like effects in adult rats, J. Neurosci. 30 (2010) 12653–12663.
[4] K. Jin, Y. Sun, L. Xie, X.O. Mao, J. Childs, A. Peel, A. Logvinova, S. Banwait, D.A. Greenberg, Comparison of ischemia-directed migration of neural precursor cells after intrastriatal, intraventricular, or intravenous transplantation in the rat, Neurobiol. Dis. (2) (2005) 366–374.
[5] S. Kelly, T.M. Bliss, A.K. Shah, G.H. Sun, M. Ma, W.C. Foo, J. Masel, M.A. Yenari, I.L. Weissman, N. Uchida, T. Palmer, G.K. Steinberg, Transplanted human fetal neural progenitor cells survive, migrate, and differentiate in ischemic rat cerebral cortex, Proc. Natl. Acad. Sci. U. S. A. 101 (2004) 11839–11844.
[6] H. Olstorn, M. Varghese, W. Murrell, M.C. Moe, I.A. Langmoen, Predifferentiated brain-derived adult human progenitor cells migrate toward ischemia after transplantation to the adult rat brain, Neurosurgery. 68 (2011) 213–222.
[7] G. Santilli, G. Lamorte, L. Carlessi, D. Ferrari, L. Rota Nodari, E. Binda, D. Delia, A.L. Vescovi, L. De Filippis, Mild hypoxia enhances proliferation and multipotency of human neural progenitor cells, PLoS One 5 (2010) e8575, , https://doi.org/10.1371/journal.pone.0008575.
[8] H.F. Bürgers, D.W. Schelshorn, W. Wagner, W. Kuschinsky, M.H. Maurer, Acute anoxia stimulates proliferation in adult neural progenitor cells from the rat brain, Exp. Brain Res. 188 (2008) 33–43.
[9] D.M. Fagel, Y. Ganat, J. Silbereis, T. Ebbitt, W. Stewart, H. Zhang, L.R. Ment, F.M. Vaccarino, Cortical neurogenesis enhanced by chronic perinatal hypoxia, Exp. Neurol. 199 (2006) 77–91.
[10] T. Nordström, L.C. Jansson, L.M. Louhivuori, K.E. Akerman, Effects of acute

hypoxia/acidosis on intracellular pH in differentiating neural progenitor cells, Brain Res. 1461 (2012) 10–23.
[11] M. Fujita, H. Asanuma, A. Hirata, M. Wakeno, H. Takahama, H. Sasaki, J. Kim, S. Takashima, O. Tsukamoto, T. Minamino, Y. Shinozaki, H. Tomoike, M. Hori, M. Kitakaze, Prolonged transient acidosis during early reperfusion contributes to the cardioprotective effects of postconditioning, Am. J. Physiol. Heart Circ. Physiol. 292 (2007) H2004–H2008.
[12] T.I. Lam, A.M. Brennan-Minnella, S.J. Won, Y. Shen, C. Hefner, Y. Shi, D. Sun, R.A. Swanson, Intracellular pH reduction prevents excitotoxic and ischemic neuronal death by inhibiting NADPH oxidase, Proc. Natl. Acad. Sci. U. S. A. 110 (2013) E4362–E4368.
[13] A.G. Mukhin, S.A. Ivanova, J.W. Allen, A.I. Faden, Mechanical injury to neuronal/glial cultures in microplates: role of NMDA receptors and pH in secondary neuronal cell death, J. Neurosci. Res. 51 (1998) 748–758.
[14] R.G. Giffard, H. Monyer, C.W. Christine, D.W. Choi, Acidosis reduces NMDA receptor activation, glutamate neurotoxicity, and oxygen-glucose deprivation neuronal injury in cortical cultures, Brain Res. 506 (1990) 339–342.
[15] P. Holzer, Acid-sensitive ion channels and receptors, Handb. Exp. Pharmacol. 194 (2009) 283–332.
[16] M. Chesler, K. Kaila, Modulation of pH by neuronal activity, Trends Neurosci. (10) (1992) 396–402.
[17] K. Beppu, T. Sasaki, K.F. Tanaka, A. Yamanaka, Y. Fukazawa, R. Shigemoto, K. Matsui, Optogenetic countering of glial acidosis suppresses glial glutamate release and ischemic brain damage, Neuron. 81 (2014) 314–320.
[18] D.L. Clarke, C.B. Johansson, J. Wilbertz, B. Veress, E. Nilsson, H. Karlström, U. Lendahl, J. Frisén, Generalized potential of adult neural progenitor cells, Science. 288 (2000) 1660–1663.
[19] T. Nordström, O.D. Rotstein, R. Romanek, S. Asotra, J.N. Heersche, M.F. Manolson, G.F. Brisseau, S. Grinstein, Regulation of cytoplasmic pH in osteoclasts. Contribution of proton pumps and a proton-selective conductance, J. Biol. Chem. 270 (1995) 2203–2212.
[20] Y. Liu, J.Y. Xu, D.K. Wang, L. Wang, L.M. Chen, Cloning and identification of two novel NBCe1 splice variants from mouse reproductive tract tissues: a comparative study of NCBT genes, Genomics 98 (2011) 112–119.
[21] L.C. Jansson, L. Louhivuori, H.K. Wigren, T. Nordström, V. Louhivuori, M.L. Castrén, K.E. Åkerman, Effect of glutamate receptor antagonists on migrating neural progenitor cells, Eur. J. Neurosci. 37 (2013) 1369–1382.
[22] V. Kärkkäinen, V. Louhivuori, M.L. Castrén, K.E. Åkerman, Neurotransmitter responsiveness during early maturation of neural progenitor cells, Differentiation. 77 (2009) 188–198.
[23] F.F. Ch'en, F.C. Villafuerte, P. Swietach, P.M. Cobden, R.D. Vaughan-Jones, S0859, an N-cyanosulphonamide inhibitor of sodium-bicarbonate cotransport in the heart, Br. J. Pharmacol. 153 (2008) 972–982.
[24] D.E. Kim, D. Schellingerhout, K. Ishii, K. Shah, R. Weissleder, Imaging of stem cell recruitment to ischemic infarcts in a murine model, Stroke 35 (2004) 952–957.
[25] M. Nedergaard, R.P. Kraig, J. Tanabe, W.A. Pulsinelli, Dynamics of interstitial and intracellular pH in evolving brain infarct, Am. J. Phys. 260 (3) (1991) R581–R588 Pt 2.
[26] G. Song, C. Li, X. Luo, X. Zhao, S. Zhang, Y. Zhang, S. Jiang, X. Wang, Y. Chen, H. Chen, T. Gong, J. Zhou, M. Chen, Evolution of cerebral ischemia assessed by amide proton transfer-weighted MRI, Front. Neurol. 8 (2017) 67, https://doi.org/10.3389/fneur.2017.00067 eCollection 2017.
[27] P. Orlowski, M. Chappell, C.S. Park, V. Grau, S. Payne, Modelling of pH dynamics in brain cells after stroke, Interface Focus 1 (2011) 408–416.
[28] S.N. Basovich, The role of hypoxia in mental development and in the treatment of mental disorders: a review, Biosci. Trends 4 (2010) 288–296.
[29] A.L. Beal, K.E. Scheltema, G.J. Beilman, W.E. Deuser, Hypokalemia following trauma, Shock. 18 (2002) 107–110.
[30] O. Wiesel, O. Szold, I. Bentov, P. Sorkin, A. Nimrod, P. Biderman, Dyskalemia following head trauma: case report and review of the literature, J. Trauma 67 (2009) E149–E151.
[31] X. Wu, X. Lu, X. Lu, J. Yu, Y. Sun, Z. Du, X. Wu, Y. Mao, L. Zhou, S. Wu, J. Hu, Prevalence of severe hypokalaemia in patients with traumatic brain injury, Injury. 46 (2015) 35–41.
[32] T. Ookuma, K. Miyasho, N. Kashitani, N. Beika, N. Ishibashi, T. Yamashita, Y. Ujike, The clinical relevance of plasma potassium abnormalities on admission in trauma patients: a retrospective observational study, J. Intensive Care (2015) 37, https://doi.org/10.1186/s40560-015-0103-6.
[33] L.C. Jansson, K.E. Åkerman, The role of glutamate and its receptors in the proliferation, migration, differentiation and survival of neural progenitor cells, J. Neural Transm. (Vienna) 12 (2014) 819–836.
[34] L.M. Louhivuori, P.M. Turunen, V. Louhivuori, V. Yellapragada, T. Nordström, P. Uhlén, K.E. Åkerman, Regulation of radial glial process growth by glutamate via mGluR5/TRPC3 and neuregulin/ErbB4, Glia 66 (2018) 94–107.
[35] L. Zhao, Q. Jiao, P. Yang, X. Chen, J. Zhang, B. Zhao, P. Zheng, Y. Liu, Metabotropic glutamate receptor 5 promotes proliferation of human neural stem/progenitor cells with activation of mitogen-activated protein kinases signaling pathway in vitro, Neuroscience. 192 (2011) 185–194.
[36] Z. Xiong, W. Lu, J.F. MacDonald, Extracellular calcium sensed by a novel cation channel in hippocampal neurons, Proc. Natl. Acad. Sci. U. S. A. 94 (1997) 7012–7017.
[37] D. Ren, Sodium leak channels in neuronal excitability and rhythmic behaviors, Neuron. 72 (2011) 899–911.
[38] P. Nilsson, L. Hillered, Y. Olsson, M.J. Sheardown, A.J. Hansen, Regional changes in interstitial K^+ and Ca^{2+} levels following cortical compression contusion trauma in rats, J. Cereb. Blood Flow Metab. 13 (1993) 183–192.
[39] W. Young, Role of calcium in central nervous system injuries, J. Neurotrauma 9 (Suppl. 1) (1992) S9–25.
[40] B. Billups, D. Attwell, Modulation of non-vesicular glutamate release by pH, Nature 379 (1996) 171–174.
[41] M. Szatkowski, B. Barbour, D. Attwell, Non-vesicular release of glutamate from glial cells by reversed electrogenic glutamate uptake, Nature. 348 (1990) 443–446.
[42] S. Paluzzi, S. Alloisio, S. Zappettini, M. Milanese, L. Raiteri, M. Nobile, G. Bonanno, Adult astroglia is competent for Na+/Ca2+ exchanger-operated exocytotic glutamate release triggered by mild depolarization, J. Neurochem. 103 (2007) 1196–1207.
[43] R.A. Kauppinen, K. Enkvist, I. Holopainen, K.E. Akerman, Glucose deprivation depolarizes plasma membrane of cultured astrocytes and collapses transmembrane potassium and glutamate gradients, Neuroscience (1) (1988) 283–289.
[44] S. Trapp, K. Ballanyi, KATP channel mediation of anoxia-induced outward current in rat dorsal vagal neurons in vitro, J. Physiol. 487 (1995) 37–50.
[45] G. Erdemli, Y.Z. Xu, K. Krnjević, Potassium conductance causing hyperpolarization of CA1 hippocampal neurons during hypoxia, J. Neurophysiol. 80 (1998) 2378–2390.
[46] M. Chesler, Regulation and modulation of pH in the brain, Physiol. Rev. 83 (2003) 1183–1221.
[47] M.L. Astion, R.K. Orkand, Electrogenic Na+/HCO3- cotransport in neuroglia, Glia 1 (1988) 355–357.
[48] B.M. Schmitt, U.V. Berger, R.M. Douglas, M.O. Bevensee, M.A. Hediger, G.G. Haddad, W.F. Boron, Na/HCO3 cotransporters in rat brain: expression in glia, neurons, and choroid plexus, J. Neurosci. 20 (2000) 6839–6848.
[49] D.S. Cooper, N.C. Saxena, H.S. Yang, H.J. Lee, A.G. Moring, A. Lee, I. Choi, Molecular and functional characterization of the electroneutral Na/HCO3 cotransporter NBCn1 in rat hippocampal neurons, J. Biol. Chem. 280 (2005) 17823–17830.
[50] L.M. Chen, M.L. Kelly, J.D. Rojas, M.D. Parker, H.S. Gill, B.A. Davis, W.F. Boron, Use of a new polyclonal antibody to study the distribution and glycosylation of the sodium-coupled bicarbonate transporter NCBE in rodent brain, Neuroscience 151 (2008) 374–385.
[51] H.J. Lee, H.J. Park, S. Lee, Y.H. Kim, I. Choi, The sodium-driven chloride/bicarbonate exchanger NDCBE in rat brain is upregulated by chronic metabolic acidosis, Brain Res. 1377 (2011) 13–20.
[52] C.J. Schwiening, W.F. Boron, Regulation of intracellular pH in pyramidal neurones from the rat hippocampus by Na(+)-dependent Cl(−)-HCO3- exchange, J. Physiol. 475 (1994) 59–67.
[53] W.R. Schlue, J.W. Deitmer, Ionic mechanisms of intracellular pH regulation in the nervous system, CIBA Found. Symp. 139 (1988) 47–69.
[54] P. Mellergård, Y.B. Ouyang, B.K. Siesjö, The regulation of intracellular pH is strongly dependent on extracellular pH in cultured rat astrocytes and neurons, Acta Neurochir. Suppl. (Wien) 60 (1994) 34–37.
[55] A. McIntyre, A. Hulikova, I. Ledaki, C. Snell, D. Singleton, G. Steers, P. Seden, D. Jones, E. Bridges, S. Wigfield, J.L. Li, A. Russell, P. Swietach, A.L. Harris, Disrupting hypoxia-induced bicarbonate transport acidifies tumor cells and suppresses tumor growth, Cancer Res. 76 (2016) 3744–3755.
[56] D.M. Panchision, The role of oxygen in regulating neural stem cells in development and disease, Cell. Physiol. 220 (2009) 562–568.
[57] M.H. Kim-Lee, B.T. Stokes, A.J. Yates, Reperfusion paradox: a novel mode of glial cell injury, Glia 5 (1992) 56–64.
[58] W. Young, Ca paradox in neural injury: a hypothesis, Cent. Nerv. Syst. Trauma 3 (1986) 235–251 (Summer).